PERGAMON

International Journal of Heat and Mass Transfer 45 (2002) 4097–4106

International Journal of HEAT and MASS TRANSFER

www.elsevier.com/locate/ijhmt

Contact melting inside an elastic capsule

Alexander V. Wilchinsky [a,*], Sergei A. Fomin [b], Toshiyuki Hashida [b]

[a] *Institute of Mathematics and Mechanics, Kazan State University, Kazan, Russia*
[b] *Fracture Research Institute, School of Engineering, Tohoku University, Sendai, Japan*

Received 28 August 2001; received in revised form 26 March 2002

Abstract

An approximate mathematical model of contact melting of an unfixed material in elastic cylindrical and spherical capsules is developed. Since the density of the solid is higher than that of the melt, the melting solid resides at the bottom supported by a thin layer of the generated, convecting, melt, and the capsule swells. The main characteristic scales and non-dimensional parameters, which describe the principal features of the melting process and the liquid flow, are found. Linearisation with regard to the Stefan number as well as the small difference between the densities of the solid and liquid enables us to derive a closed-form evolution equation for the motion of the solid, which also determines the melting rate. Numerical solution of the evolution equation shows that the swelling of the capsule during melting, which is caused by the decrease of the density during phase transition, leads to slowing down of the melting process. This effect is due to flattening of the lower surface of the capsule, which entails fall of the pressure along with thickening of the molten layer. The latter determines the decrease of the melting rate. © 2002 Published by Elsevier Science Ltd.

1. Introduction

Analysis of close-contact melting of a solid in a cavity is motivated by application in latent heat-of-fusion thermal-storage systems. Contact melting in a circular horizontal cylinder has been studied numerically by Saitoh and Hirose [1] and Nicholas and Bayazitoglu [2], where the energy equation was solved in a thin molten layer, which determined the sinking velocity of the solid core. Analytical solution was found by Bareiss and Beer [3], who showed its good agreement with experimental results for small Stefan numbers. Contact melting in a spherical capsule was investigated numerically by Moore and Bayazitoglu [4] and later, applying the technique proposed in [3], Bahrami and Wang [5], Roy and Sengupta [6] as well as Fomin and Saitoh [7] reported analytical solutions. Fomin et al. [8] studied the effect of the shape factor of elongated capsules on the melting rate. The general scheme for the scale analysis of the contact melting problem was proposed by Bejan [9]. Although the aforementioned investigations highlight the main characteristics of contact melting inside a capsule, the effect of the difference between the densities of the solid and liquid phase, which leads to swelling of the capsule, has not been yet analysed. In the present paper the approximate approach developed by Bareiss and Beer [3] is applied with the higher order of accuracy with regard to non-linear temperature distribution in the melt, accounting for the convective heat transfer, for the mathematical modelling of contact melting in elastic horizontal circular cylinder and sphere. The main objective of the work is to derive a closed-form evolution equation for the solid motion and estimate the effect of the capsule swelling on the melting rate.

2. System model and analysis

Melting process within a circular capsule is illustrated in Fig. 1. The equation $(x^*/a)^2 + (y^*/a)^2 = 1$ describes the generating curve of the internal surface of the capsule which can be a horizontal circular cylinder or a sphere completely filled with solid phase. In the first case (x^*, y^*) are Cartesian coordinates, and in the second case

* Corresponding author. Present address: Department of Space and Climate Physics, University College London, Gower Str., London, WC1E 6BT, UK. Fax: +44-20-7679-7883.
E-mail address: aw@cpom.ucl.ac.uk (A.V. Wilchinsky).

0017-9310/02/$ - see front matter © 2002 Published by Elsevier Science Ltd.
PII: S0017-9310(02)00121-7

Nomenclature

a, a_{ext}	the internal and external radii of the sphere or circular cylinder containing only the solid phase
b	the internal radius of the swelled sphere or circular cylinder containing the solid and liquid phases
c_s, c_l	specific heat of the solid and liquid, respectively
e^*	the radial displacement of the capsule's shell
E	Young's modulus of the capsule's shell
g	gravitational acceleration
h	the non-dimensional molten layer thickness
H	the normalised thickness of the capsule's shell, $= (a_{ext} - a)/a$
$\overline{h}$	projection of the thickness h on the vertical, y-direction
k_s, k_l	the solid and liquid heat conductivities
l	the tangential coordinate, $= l^*/a$, as shown in Fig. 1
L_m	the melting latent heat
n	the transverse coordinate, $= n^*/h^*$, as shown in Fig. 1
$\overline{p}$	the liquid pressure
p	the excess liquid pressure, $= (\overline{p}^* - \rho_l g(a - y^*) - p^*_{min})/p_0$
p^*_{min}	is the minimum pressure in the capsule
r^*	the radial coordinate in spherical or cylindrical coordinate system
s	the shift of the reference point fixed in the solid core with regard to the bottom of the capsule (Fig. 1), $= s^*/2a$
$\dot{s}$	melting rate, $= \mathrm{d}s/\mathrm{d}\tau$
Ste	Stefan number, $= c_l(T_{w0} - T^*_m)/L_m$
T	the non-dimensional liquid temperature
T^*_m	the dimensional melting temperature
T_w	the non-dimensional wall temperature
T_{w0}	the characteristic wall temperature
u, w	dimensionless tangential and transverse velocities
V^*	the volume of the solid (taken per unit width in the case of cylinder)
V_v	dimensionless normalised volume of the solid, $= V^*/(2\pi^v a^{v+2})$
x	the dimensionless horizontal coordinate, $= x^*/a$
y	the dimensionless vertical coordinate, $= y^*/a$

Greek symbols

ε	the ratio of the molten layer thickness scale to the capsule radius, $= h_0/a$
ϵ^*_{ij}	the strain tensor in the capsule's shell
δ	the relative elongation of the capsule radius, $= (b - a)/a$
δ_{ij}	the unit tensor
δ_{max}	the maximal elongation of the capsule radius (attained when the capsule contains only liquid), $= (\rho_s/\rho_l)^{1/(v+2)} - 1$
δ_ρ	the relative difference between the solid and liquid densities, $= (\rho_s - \rho_l)/\rho_l$
μ	the liquid viscosity
$v = 0, 1$	parameter determining if a circular cylinder or a sphere is considered
φ	is the angular coordinate in spherical or cylindrical coordinate system
ρ_s, ρ_l	the constant densities of the solid and liquid
σ	the Poisson's ratio
σ^*_{ij}	the stress tensor acting in the capsule's shell
σ^*_t	the tensile strength of the capsule's shell
$\theta = (n, y)$	the angle between the vertical axis and the internal normal to the capsule wall, as shown in Fig. 1;
τ	the non-dimensional time
τ_m	the time required to complete melting of the solid core

Superscript

*	dimensional quantity

Subscripts

l	liquid
m	melting
s	solid
w	wall of the capsule
0	scales
e	marginal point of the molten layer

(x^*, y^*) are cylindrical coordinates, where x^* is the radial distance and y^* is the axis of symmetry. The capsule's shell generally has finite thickness and is linearly elastic. Initially, the circular capsule contains material in solid phase, which occupies the full space of the capsule. Then the wall temperature is raised to the value $T^*_w > T^*_m$ and is held at this value during the period necessary to melt the solid completely. The unfixed solid bulk sinks [1] because its density is higher than that of the molten liquid. The melting of the solid and its downward motion is characterised by the time-dependent shift s^* of a material-

[1] We do not treat ice.

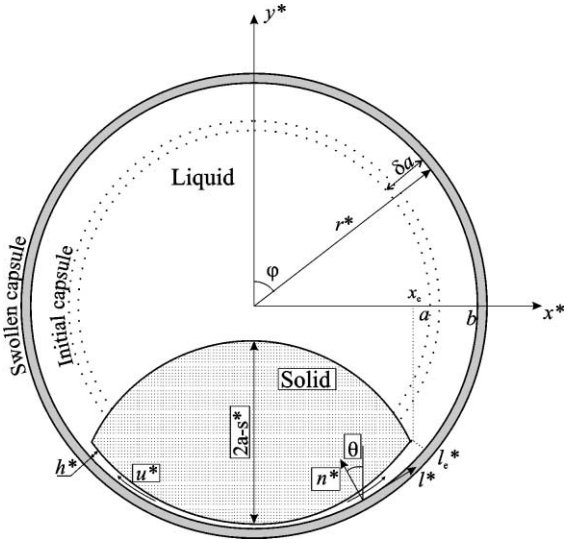

Fig. 1. The cross-section of an elastic capsule of circular cross-section containing a melting unfixed solid.

fixed reference point, which is chosen to be the centre of the core, about the bottom of the capsule (Fig. 1). In case of a rigid capsule, s^* describes the vertical shift of the solid core. The motion of the solid bulk is accompanied by the generation of liquid at the melting surface. This liquid is squeezed up to the space above the solid through a narrow gap between the melting surface and the wall of the capsule. At the same time, because the density of the liquid is smaller than that of the solid, the capsule swells.

Conventionally, the solid–liquid interface can be divided into two parts by the time-dependent value l_e of the tangential coordinate (Fig. 1): the bottom interface ($l < l_e$), which represents the close-contact melting area, where most of the intensive melting occurs, and the upper interface, where much slower "latent" melting takes place. Experiments on melting in a circular horizontal tube conducted by Bareiss and Beer [3] showed that the thickness of the molten layer in the close-contact area is considerably smaller than the characteristic size of the cavity, and the melting at the upper surface of the solid is negligible because its typical amount relates to the melt generated by close-contact melting as the ratio of the typical molten layer thickness to the capsule radius $h_0/a \ll 1$. Moreover, in these experiments the upper surface of the solid core was very insignificantly changing its shape with time and, therefore, in the model the shape of this surface could be considered as approximately the same throughout the entire process.

Apart from the mentioned simplifications, we will restrict ourselves by considering the case when the liquid density is constant, and, as a particular case, we will assume the difference between the solid and liquid densities to be small. Furthermore, the capsule cross-section will be considered to be circular at any time of the process, which is the case when, during the melting, the mean liquid pressure inside the capsule is much higher than its vertical change due to the gravity force.

On the basis of all the said above, the primary assumptions made in the present study are the following:

(1) Melting at the upper surface of the solid core is negligibly small.
(2) The solid core is at the melting point.
(3) Thermophysical properties of the materials are constant.
(4) The pressure at the upper interface between the solid and liquid is hydrostatic.
(5) Since the thickness of the liquid layer in the close-contact area is very small in comparison with the dimensions of the capsule, lubrication approximation can be implemented for mathematical modelling of the heat and mass transfer processes in the molten layer. Therefore, the local two-dimensional curvilinear orthogonal coordinate system (l, n), which is often used in boundary layer problems, is applied as shown in Fig. 1.
(6) The motion of the liquid and the solid is slow, and, therefore, non-inertial.
(7) The cross-section of the capsule is always circular.

2.1. Governing equations

The curvilinear coordinate system (l^*, n^*) is chosen in such a way that, after normalisation, the transverse coordinate $n = 0$ determines the capsule wall and $n = 1$ determines the solid–liquid interface [10,11]. For the case under consideration we choose the scales for the longitudinal and transverse coordinates, temperature, excess pressure and longitudinal velocity as

$$s_0 = 2a, \quad l_0 = a, \quad n_0 = h_0, \quad T_0 = T_{w0} - T_m^*,$$

$$p_0 = ag(\rho_s - \rho_l), \quad u_0 = aw_0/h_0.$$

Here, T_{w0} is a characteristic temperature of the wall of the capsule. The characteristic excess pressure p_0 is taken as the typical difference between the gravitational and buoyancy forces acting on the solid per unit area of its surface, which must be balanced by the pressure rise over its hydrostatic value in order to keep the solid floating. The other scales will be determined from investigation of the governing equations. Henceforth, we will assume the non-dimensional melting temperature to be zero, $T_m = 0$.

2.1.1. Dynamics of the liquid

On the basis of assumption (5), the conservation equations of mass, momentum and energy in dimensionless form can be written as

$$\frac{\partial w}{\partial n}+\frac{1}{x^v}\frac{\partial (x^v h u)}{\partial l}=0,\quad x=b\sin\theta,\quad v=0,1, \tag{1}$$

$$\frac{\partial p}{\partial l}=\frac{\eta}{h^2}\frac{\partial^2 u}{\partial n^2},\quad \eta=\frac{\mu u_0 a}{p_0 h_0^2}, \tag{2}$$

$$\frac{\partial p}{\partial n}=0, \tag{3}$$

$$Ste\left(u\frac{\partial T}{\partial l}+\frac{w}{h}\frac{\partial T}{\partial n}\right)=\frac{1}{h^2}\frac{\partial^2 T}{\partial n^2}, \tag{4}$$

where $v=0$ corresponds to the circular cylinder and $v=1$ corresponds to the sphere. These are essentially the lubrication equations with an accuracy $O(\varepsilon)$ expressed in curvilinear coordinates. Here the terms of $O(\varepsilon)$ are neglected since the parameter $\varepsilon=h_0/a$, which represents the ratio of the gap-width scale to the characteristic dimension of the capsule, is very small and varies in the range 10^{-3}–10^{-2} for different phase-change materials used in thermal-storage systems. Eq. (1) is the mass balance, (2) and (3) express the longitudinal and normal force balance, and (4) is the steady-state energy balance. To order $O(\varepsilon)$, the Stefan condition at the solid–liquid interface, $n=1$, yields

$$w=\left[\frac{\varphi}{h}\frac{\partial T}{\partial n}\right]_{n=1},\quad \varphi=\frac{k_l(T_{w0}-T_m^*)}{h_0\rho_l L_m w_0}. \tag{5}$$

To the same order of accuracy, the transverse velocity at the solid–liquid interface $n=1$ can also be found as

$$w=-\sigma\dot{s}\cos\theta,\quad \sigma=\frac{2\rho_s a}{\rho_l w_0\tau_0}. \tag{6}$$

From (3) it can be seen that p is a function of only one independent variable l. Equating $\eta=1$ in (2), $\varphi=1$ in the Stefan condition (5) and $\sigma=1$ in (6) yields the scales for the molten layer thickness, transverse velocity and time as follows

$$h_0^4=\frac{a(T_{w0}-T_m)\mu k_l}{L_m\rho_l g(\rho_s-\rho_l)},\quad w_0=\frac{k_l(T_{w0}-T_m^*)}{\rho_l h_0 L_m},\quad \tau_0=\frac{2a\rho_s}{w_0\rho_l}. \tag{7}$$

Because the typical time scale for the solid is $\rho_s c_s a^2/k_s$, assumption (2) requires

$$\frac{\rho_s c_s a}{k_s}\ll\frac{2\rho_s}{w_0\rho_l}, \tag{8}$$

while assumptions (1) and (5) are adequate when $\varepsilon=h_0/a\ll 1$.

Integrating the momentum equation (2) twice with respect to n and taking into account the no-slip conditions on both the capsule wall and melting interface, we can find the expression for the longitudinal velocity

$$u=\frac{h^2}{2}\frac{\partial p}{\partial l}(n^2-n). \tag{9}$$

Substituting the expression for the longitudinal velocity (9) into the continuity equation (1), integrating with respect to n and l, and taking into account the boundary condition (6) and the impermeability condition on the wall of the capsule, we derive the expressions for the pressure gradient and the transverse velocity

$$\frac{\partial p}{\partial l}=-\frac{12x\dot{s}}{(v+1)h^3}, \tag{10}$$

$$w=\dot{s}\cos\theta(2n^3-3n^2). \tag{11}$$

2.1.2. Dynamics of the solid

Balancing the forces acting on the solid in the vertical direction, namely the gravitational force and the force exerted by the liquid, yields with an accuracy of $O(\varepsilon)$

$$\int_0^{x_e} p x^v\,dx=V_v(s),\quad v=1,0, \tag{12}$$

where the normalised solid volumes for the cylinder, $V_0=V^*/(2a^2)$, and sphere, $V_1=V^*/(2\pi a^3)$, are given respectively as

$$2V_0=\arcsin x_e+x_e\sqrt{1-x_e^2}+\frac{b^2}{a^2}\arcsin\frac{a x_e}{b}+\frac{b}{a}x_e\sqrt{1-\frac{a^2x_e^2}{b^2}}-2(2s+\delta)x_e, \tag{13}$$

$$3V_1=1-(1-x_e^2)^{3/2}-\frac{3}{2}x_e^2(2s+\delta)-\left(\frac{b^2}{a^2}-x^2\right)^{3/2}+\frac{b^3}{a^3}, \tag{14}$$

and the marginal points are given by

$$y_e=\frac{1-b^2/a^2}{2(2s+\delta)}-s-\frac{\delta}{2},\quad x_e=\sqrt{\frac{b^2}{a^2}-y_e^2}.$$

The magnitude of the gravitational force at the right-hand side of Eq. (12) depends on the solid bulk volume which varies with time since s is a function of time. As it can be seen from Eqs. (13) and (14), at the final stage of the melting process, when s tends to 1, the volume of the solid bulk and, therefore, the magnitude of the gravitational force vanish to zero. At the left-hand side of Eq. (12), the force acting in the direction opposite to the gravitational force is represented by the force of pressure in the liquid layer. The other component of this force caused by the shear stresses is ignored since its magnitude is of order $O(\varepsilon)$.

Using the expression for the pressure gradient (10) we can rewrite the force balance equation (12) in the form

$$\frac{12\dot{s}}{(v+1)^2}\int_0^{x_e}\frac{x^{v+2}}{h^3\cos\theta}\,dx=V_v,\quad v=0,1. \tag{15}$$

In case of a small expansion of the capsule δ caused by a small difference between the solid and liquid densities, to order of $O(\delta^2)$ we can write

$$V_v = F_v + \delta G_v, \tag{16}$$

where

$$F_0 = \arccos s - s\sqrt{1-s^2}, \quad G_0 = \arccos s - \sqrt{1-s^2}, \tag{17}$$

$$F_1 = \frac{2}{3} - s + \frac{s^3}{3}, \quad G_1 = \frac{1}{2} - s + \frac{s^2}{2}, \tag{18}$$

and

$$x_e = x_{e0} + \delta x_{e1}, \tag{19}$$

where

$$x_{e0} = \sqrt{1-s^2}, \quad x_{e1} = \frac{1-s}{2\sqrt{1-s^2}}. \tag{20}$$

2.1.3. Dynamics of the capsule form

Because the liquid density is constant, in order to find the measure of the expansion of the capsule, δ, we can consider the balance of mass, which can be written for the circular cylinder and the sphere as

$$\frac{\pi\delta_\rho}{2} = V_0\delta_\rho + \frac{\pi}{2}\left(\frac{b^2}{a^2} - 1\right), \quad v = 0, \tag{21}$$

$$\frac{2\delta_\rho}{3} = V_1\delta_\rho + \frac{2}{3}\left(\frac{b^3}{a^3} - 1\right), \quad v = 1, \tag{22}$$

where $\delta_\rho = (\rho_s - \rho_l)/\rho_l$. When values of δ are not small, then the above equations for the mass balance, together with expressions (13) and (14) for V_v, constitute a nonlinear system of algebraic equations for determination of the functions $V_v(s)$ and $\delta(s) = b/a - 1$, which, however, are difficult to solve analytically in general case. For small values of δ, we can use linearisation with regard to δ. In this case, to order $O(\delta^2)$ the mass balance yields

$$\delta = \delta_\rho\left(\frac{1}{2} - \frac{V_0}{\pi}\right), \quad v = 0, \tag{23}$$

$$\delta = \delta_\rho\left(\frac{1}{3} - \frac{V_1}{2}\right), \quad v = 1. \tag{24}$$

Taking into account (16), we derive the expressions for the relative elongation of the capsule radius

$$\delta = \delta_\rho\left(\frac{1}{2} - \frac{F_0}{\pi}\right) + O(\delta_\rho^2), \quad v = 0, \tag{25}$$

$$\delta = \delta_\rho\left(\frac{1}{3} - \frac{F_1}{2}\right) + O(\delta_\rho^2), \quad v = 1. \tag{26}$$

2.2. Simplified model of close-contact melting

As it was already mentioned, the derivation of the mathematical model presented above is based on the fact that the parameter $\varepsilon = h_0/a \sim 10^{-3}$–$10^{-2}$, therefore values of order $O(\varepsilon)$ are ignored. This model is governed by another small parameter—the Stefan number. For a number of situations and a variety of phase-change materials $Ste < 0.5$. The latter allows us to implement the perturbation methods and to neglect in the further analysis the terms of the order of $O(Ste^2)$. Within the bounds of the adopted accuracy, the temperature profile, which should be substituted into the left-hand side of Eq. (4), can be taken as follows

$$T = T_w(1-n) + O(Ste). \tag{27}$$

From the Stefan condition (5) and Eq. (27), it also follows that

$$T_w = h\dot{s}\cos\theta + O(Ste). \tag{28}$$

Due to Eq. (28), we can express the molten layer thickness at leading order as $h = T_w/(\dot{s}\cos\theta) + O(Ste)$. Taking this into account, and using the linear approximation for the temperature (27) with the expression for the velocities (9) and (11) in the convective parts of the energy balance (4), we can rewrite the last as

$$-Ste\,h\dot{s}\cos\theta\left[\frac{6x}{(v+1)\cos\theta}\frac{\partial T_w}{\partial l}(n^2-n)(1-n) + (2n^3-3n^2)T_w\right] = \frac{\partial^2 T}{\partial n^2} + O(Ste^2). \tag{29}$$

After integration of this equation twice, from n to 1 and from 0 to n, and taking into account the boundary conditions at the melting interface (5) and (6) and the wall, we derive the temperature distribution

$$T = T_w + Ste\,h\dot{s}\cos\theta\left[\frac{6x}{(v+1)\cos\theta}\frac{\partial T_w}{\partial l}\left(\frac{n^5}{20} - \frac{n^4}{6} + \frac{n^3}{6} - \frac{n}{12}\right) + \left(\frac{n^4}{4} - \frac{n^5}{10} - \frac{n}{2}\right)T_w\right] - nh\dot{s}\cos\theta + O(Ste^2). \tag{30}$$

Equating the temperature at the melting surface, $n = 1$, to zero, we can find the molten layer thickness to order of $O(Ste^2)$

$$h = \frac{T_w}{\dot{s}\cos\theta}\left[1 - Ste\left(\frac{x}{5(v+1)\cos\theta}\frac{\partial T_w}{\partial l} + \frac{7}{20}T_w\right)\right]. \tag{31}$$

If the temperature distribution on the wall of the capsule, $T_w(l)$, is given, then (31) and the force balance equation (15) constitute an integro-differential system, from which the shift of the solid core, $s = s(\tau)$, and the thickness of the molten layer, $h = h(l,\tau)$, can be determined. For an arbitrary T_w, this system of equations can

be solved numerically, however, the closed-form analytical solution can be readily obtained, provided that the temperature on wall is constant at a fixed time, $\partial T_w/\partial l \equiv 0$. In this case, the product $\overline{h} = h\cos\theta$ does not depend on x and can be a function of the time only, given by the expression

$$\overline{h}\dot{s} = T_w(1 - 7SteT_w/20). \tag{32}$$

As a result, the force balance equation (15) reduces to

$$\bar{h}^3 = \frac{12\dot{s}\Gamma_v}{(v+1)^2 V_v}, \tag{33}$$

where

$$\Gamma_v = \int_0^{x_e} x^{v+2}\cos^2\theta\,\mathrm{d}x = \frac{x_e^{v+3}}{v+3} - \frac{a^2 x_e^{v+5}}{b^2(v+5)}. \tag{34}$$

To order of $O(\delta^2)$ we can write

$$\Gamma_v = \Phi_v + \delta\Psi_v, \tag{35}$$

where

$$\Phi_v = \frac{x_{e0}^{v+3}}{v+3} - \frac{x_{e0}^{v+5}}{v+5}, \quad \Psi_v = x_{e1}x_{e0}^{v+2}(1-x_{e0}^2) + \frac{2x_{e0}^{v+5}}{v+5}. \tag{36}$$

Now, the pressure distribution can be found from (10) as

$$p = \frac{3\dot{s}}{(v+1)\bar{h}^3}\left(2x_e^2 - \frac{a^2}{b^2}x_e^4 - 2x^2 + \frac{a^2}{b^2}x^4\right), \tag{37}$$

which, to order of $O(\delta^2)$, yields

$$p = \frac{3\dot{s}}{(v+1)\bar{h}^3}\left\{1 - s^4 - 2x^2 + x^4 + 2\delta\left[1 - s^2 - s^3 + s^4 - x^4\right]\right\}, \tag{38}$$

where, at leading order, δ is given by (25) and (26).

Substituting expression for the molten layer thickness (32) into the force balance equation (33) leads to the evolution equation for the melted part of the solid, s,

$$\dot{s} = \left[(v+1)^2 V_v T_w^3(1 - 7Ste\,T_w/20)^3/(12\Gamma_v)\right]^{1/4}, \tag{39}$$

which is an ordinary first-order differential equation, and, in general case, V_v and Γ_v are given implicitly by (13), (14), (21), (22), (34).

If the wall temperature is constant not only along the capsule wall, but also with regard to time, then we can eliminate the factor at the right-hand side of (39) depending on T_w and Ste by rescaling the time τ

$$\tilde{\tau} = \tau\left[(v+1)^2 T_w^3(1 - 7SteT_w/20)^3/12\right]^{1/4}. \tag{40}$$

After this, due to (25) and (26), to order $O(\delta_\rho^2)$, we derive

$$\mathrm{d}s/\mathrm{d}\tilde{\tau} = \left(\frac{F_v}{\Phi_v}\right)^{1/4}\left[1 + \delta_\rho\frac{\Omega_v}{4}\left(\frac{G_v}{F_v} - \frac{\Psi_v}{\Phi_v}\right)\right], \tag{41}$$

where

$$\Omega_0 = \frac{1}{2} - \frac{F_0}{\pi}, \quad \Omega_1 = \frac{1}{3} - \frac{F_1}{2}. \tag{42}$$

Because, generally $\mathrm{d}s/\mathrm{d}\tilde{\tau}$ depends only on δ_ρ, even if it is not small, the knowledge of the function $s(\tilde{\tau})$ when δ_ρ is fixed, which can be also found from experiments for a certain value of the capsule radius and material, enables us to find solution of the problem for all quantities of the capsule radius, wall temperature and material properties with the same value of δ_ρ.

Let us now find how the time of complete melting of a certain material changes if the initial radius of the capsule and wall temperature change. Because $\mathrm{d}s/\mathrm{d}\tilde{\tau}$ does not change in this case, we derive

$$\tau_{m2}^* = \left(\frac{a_2}{a_1}\right)^{5/4}\left[\frac{T_{w1}(1 - 7Ste\,T_{w1}/20)}{T_{w2}(1 - 7Ste\,T_{w2}/20)}\right]^{3/4}\tau_{m1}^*, \tag{43}$$

where the indices point at different values of the capsule radius and wall temperature. If the wall temperature is the same, then the time of complete melting increases as power 5/4 of the radius ratio.

Since the left-hand side of Eq. (4) is a value of $O(Ste)$ and the parameter Ste is small, the heat transport between the solid and the capsule wall is dominated by conduction in the transverse direction. Nevertheless, it is advantageous to introduce the Nusselt number, in order to describe the effect of the heat convection in the molten layer for a constant wall temperature. The Nusselt numbers at the wall of the capsule, Nu_w, and at the melting interface, Nu_m can be defined as

$$Nu_w = \frac{1}{T|_{n=1} - T_w}\left.\frac{\partial T}{\partial n}\right|_{n=0}, \quad Nu_m = \frac{1}{T|_{n=1} - T_w}\left.\frac{\partial T}{\partial n}\right|_{n=1}. \tag{44}$$

Taking into account the temperature distribution (30) and neglecting the terms of order Ste^2, we derive

$$Nu_w = 1 + \frac{3}{20}Ste\,T_w, \quad Nu_m = 1 - \frac{7}{20}Ste\,T_w. \tag{45}$$

For $Ste = 0.1$, we have corrections of 1.5% and 3.5% respectively, which means that in this case the heat flux at the wall can be satisfactorily approximated by the linear interpolation of the temperature distribution. For larger values of the Stefan number, however, the linear approximation will be too rough, and the corrections are necessary to include.

2.3. Stresses acting on the capsule's shell

Let us now find stresses acting on the capsule's shell. This will enable us to find conditions guaranteeing satisfaction of assumption (7) and absence of ruptures of the capsule.

We consider a linear elastic rheology of the capsule's shell [12]

$$\sigma^*_{ij} = \frac{E}{1+\sigma}\left(\epsilon^*_{ij} + \frac{\sigma}{1-2\sigma}\epsilon^*_{kk}\delta_{ij}\right). \tag{46}$$

Let us denote $R = a_{\rm ext}/a$, where a, $a_{\rm ext}$ the internal and external radii of the undeformed capsule. Evidently, assumption (7) requires $p_{\min} \gg \rho_{\rm s} g a$ during the melting, namely when $\delta/\delta_{\max} \simeq 1$, where $\delta_{\max} = (\rho_{\rm s}/\rho_{\rm l})^{1/(v+2)} - 1$ is the maximal elongation of the capsule radius, achieved when the capsule contains only the liquid phase. At the same time, at the beginning of the melting, when $\delta/\delta_{\max} \ll 1$, volume of the melt is so small that the deformation of the capsule's shell is negligible.

The radial displacement e^* of a uniform deformation of a circular cylinder and spherical capsule depends only on the radius r^* [12]

$$e^* = \alpha r^* + \frac{\beta}{r^{*v+1}}. \tag{47}$$

The constants α, β are determined from the conditions that at the internal surface of the capsule's shell, $r^* = a$, the displacement is equal to $b - a$, and the radial stress σ^*_{rr} is equal to zero at the external surface of the capsule. This yields

$$\begin{aligned} \alpha &= \frac{2^v(1-2\sigma)}{(1+\sigma)^v a_{\rm ext}^{v+2}}\beta, \\ \beta &= \frac{(1+\sigma)^v R^{v+2}\left(\frac{b}{a}-1\right)}{2^v(1-2\sigma)+(1+\sigma)^v R^{v+2}}. \end{aligned} \tag{48}$$

For the strains in cylindrical ($v = 0$) and spherical ($v = 1$) coordinates respectively we have

$$\epsilon^*_{rr} = \alpha - \frac{2^v\beta}{r^{*v+2}}, \quad \epsilon^*_{\varphi\varphi} = \alpha + \frac{\beta}{r^{*v+2}}, \tag{49}$$

which yields for the stresses

$$\begin{aligned} \sigma^*_{rr} = {} & \frac{2^v E}{(1+\sigma)^{1-v}} \frac{R^{v+2}\delta}{2^v(1-2\sigma)+(1+\sigma)^v R^{v+2}} \\ & \times \left[1 - \left(\frac{a_{\rm ext}}{r^*}\right)^{v+2}\right], \end{aligned} \tag{50}$$

$$\begin{aligned} \sigma^*_{\varphi\varphi} = {} & \frac{E}{(1+\sigma)^{1-v}} \frac{\delta}{2^v(1-2\sigma)+(1+\sigma)^v R^{v+2}} \\ & \times \left[2^v + \left(\frac{a_{\rm ext}}{r^*}\right)^{v+2}\right]. \end{aligned} \tag{51}$$

The stresses have maximum values at the internal surface.

Because $p^*_{\min} = -\sigma^*_{rr}|_{r^*=a}$, assumption (7), neglecting the influence of the pressure change inside the capsule on the capsule form, requires in terms of scales

$$E\delta_{\max}\left(R^{v+2} - 1\right) \gg \rho_{\rm s} g a, \tag{52}$$

while the condition of intactness of the capsule yields exactly

$$\frac{E}{(1+\sigma)^{1-v}} \frac{\delta_{\max}(2^v + R^{v+2})}{2^v(1-2\sigma)+(1+\sigma)^v R^{v+2}} < \sigma^*_{\rm t}. \tag{53}$$

In case of small thickness of the capsule's shell, namely when $a_{\rm ext} = a(1+H), H \ll 1$, the above formulas yield at leading order

$$E\delta_{\max} H \gg \rho_{\rm s} g a, \quad \frac{E\delta_{\max}}{(1+\sigma)^{1-v}(1-\sigma)} < \sigma^*_{\rm t}, \tag{54}$$

with $\delta_{\max} = (\rho_{\rm s}/\rho_{\rm l})^{1/(v+2)} - 1$. Assuming the Poisson's ratio to be between 0.3 and 0.5, these estimates also give the restriction on the relative capsule thickness

$$H \gg \rho_{\rm s} g a/\sigma^*_{\rm t}. \tag{55}$$

Therefore, the capsule's wall can be thin only when both Young's modulus and tensile stress are sufficiently large, otherwise either the capsule form will be not spherical due to the non-uniform pressure distribution or the capsule's shell will be ruptured.

3. Results and discussion

Among the different phase-change materials used in the thermal energy storage systems, paraffin is most frequently used. Numerical computations, provided below, were performed for $Ste = 0.1$, and $T_{\rm w} = 1$. Results for other values of Ste can be derived by rescaling of the variables. While paraffin is characterised by $\delta_\rho = 0.185$, in order to accentuate differences in the melting regime caused by the swelling of the capsule, we will use the value $\delta_\rho = 0.3$ as a possible maximum. Solutions of the problem with other values of this parameter can be derived by linear interpolation because of the linearity of the model with regard to δ_ρ.

In order to present results of calculations for the cylinder and sphere in a unified time-coordinate, we will use the time variable $\bar\tau = \tilde\tau/\sqrt{v+1}$, whose scaling does not depend if the cylinder or the sphere is considered. Evidently, since for a cylinder and a sphere the volume of the capsule relates to its surface as $1/2a$ and $1/3a$, respectively, the melting rate of the cylinder is lower than that of the sphere, as was also confirmed by computations.

The melting rate $\mathrm{d}s/\mathrm{d}\bar\tau$ is shown in Fig. 2, from which it can be seen that the melting rate decreases during the melting. At the beginning of the melting, the melting rates for the swelling and non-swelling capsules are the same. Then the melting rate for the swelling capsule decreases in comparison with that of the non-swelling one, and their difference $\Delta\dot s$, shown in Fig. 3, reaches its maximum near the middle of the melting process. At the end, however, the difference between the melting rates

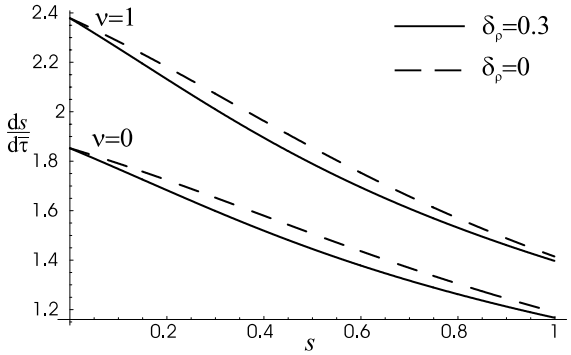

Fig. 2. The rate of melting $ds/d\bar{\tau}$ with respect to the relative solid displacement, s, for the cylinder ($v = 0$) and the sphere ($v = 1$). Solid lines show the swelling capsule ($\delta_\rho = 0.3$), while the dashed lines illustrate melting within non-swelling one ($\delta_\rho = 0$).

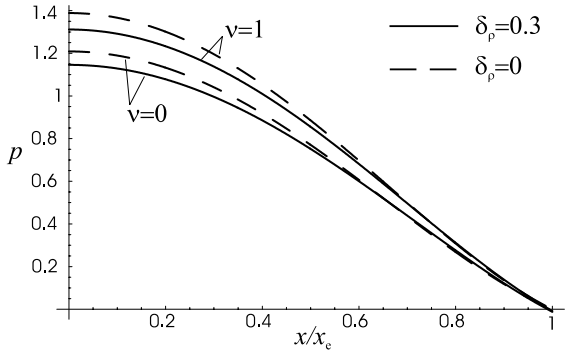

Fig. 4. The pressure distribution along the axis x for the cylinder ($v = 0$) and sphere ($v = 1$) in the middle of the melting, which corresponds to $s = 0.5$. Solid lines illustrate pressure variation in the swelling capsule ($\delta_\rho = 0.3$), while the dashed lines show the pressure when swelling is ignored ($\delta_\rho = 0$).

decreases. Such a behaviour is caused by the change of the melting-surface geometry during the melting because of the following.

The solid is supported by the pressure acting on its lower surface. As the pressure distribution along the capsule wall shows (Fig. 4), the region of the largest acting pressure, supporting the most of the solid, is there, where the melting surface is close to horizontal, because the stress acting on the solid is directed there almost vertically to counteract the gravity force. Supporting the solid at higher slopes of the contact surface would require much higher pressure there, which would lead to a negative pressure gradient along the wall, hampering the melt outflow. Then, the smaller the flat horizontal area is, the larger will be the pressure necessary to support the solid, and, hence, the smaller will be the molten layer thickness, which yields the higher melting rate. Furthermore, because the solid mass decreases during the melting, the pressure also decreases (Fig. 5), which leads to increasing of the molten layer thickness accompanied by the decrease of the melting rate of both capsules during the melting.

Let us now turn to the difference in the melting rate in the capsules. At the beginning of the melting, both capsules have the same form, and, therefore, the same melting rate. During the melting, the contact surface of the swelling capsule flattens, which leads to the higher decrease of the pressure (Fig. 5) and to the higher decrease of the melting rate. Close to the end of the melting, when $x_1 \to 0$, the contact-surface slope of the

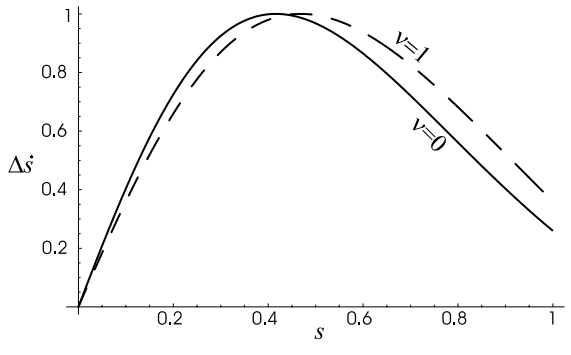

Fig. 3. Variation of the normalised difference between the melting rates of the swelling and non-swelling capsules, $\Delta\dot{s} = (ds/d\bar{\tau}|_{\delta_\rho=0} - ds/d\bar{\tau}|_{\delta_\rho=0.3})/(ds/d\bar{\tau}|_{\delta_\rho=0} - ds/d\bar{\tau}|_{\delta_\rho=0.3})|_{\max}$, during the melting vs the relative solid displacement, s. The solid and dashed lines represent respectively melting within the cylinder ($v = 0$) and sphere ($v = 1$).

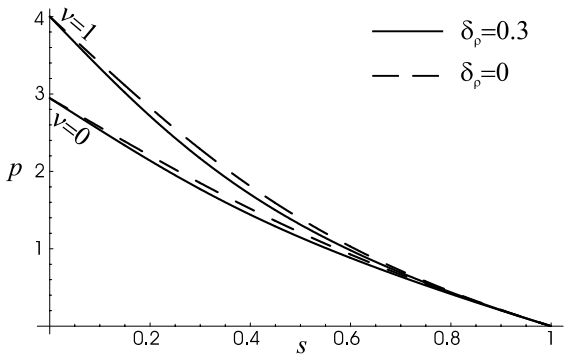

Fig. 5. The dynamics of the pressure at the bottom during the melting vs the relative solid displacement, s, in the cylinder ($v = 0$) and sphere ($v = 1$). Solid lines describes the process in the swelling capsule ($\delta_\rho = 0.3$), while the dashed lines – in the rigid one when non-swelling is ignored ($\delta_\rho = 0$).

solids in both capsules tends to zero, which diminishes the difference in their melting rate.

The change of the time of complete melting of the solid, $\bar{\tau}_m$, is shown in Fig. 6. Because the model is linear, it gives linear increase of the complete-melting time with increasing δ_ρ. The calculations give the rate of this increase as $d\bar{\tau}_m/d\delta_\rho = 0.0697$ for the cylinder and $d\bar{\tau}_m/d\delta_\rho = 0.047$ for the sphere. The time of complete melting increases faster for the cylinder than for the sphere because the maximum elongation of the capsule radius δ_{max} for the same density difference is higher for the cylinder than for the sphere.

The normalised elongation of the capsule radius δ/δ_{max} is shown in Fig. 7. Generally, the rate of swelling decreases with s, because the surface of contact melting has maximum area at the beginning, which then decreases during the melting. The rate of the increase of the capsule radius, equal to $(4/\pi)\sqrt{1-s^2}$ for the cylinder and $(3/2)(1-s^2)$ for the sphere, is higher for the sphere during the beginning of the melting, when $s < \sqrt{1-4/9\pi^2}$, and lower later. Because the volume of the cylinder is proportional to a^2, while that of the sphere to a^3, an initial decrease of the radius of the solid,

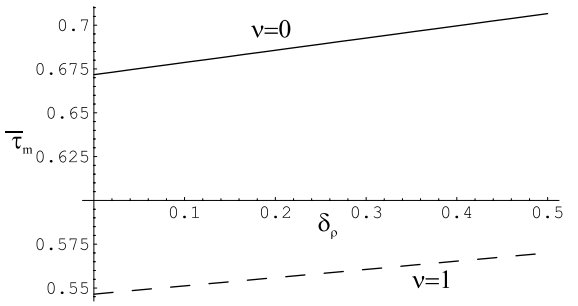

Fig. 6. The time of complete melting of the solid, $\bar{\tau}_m$, vs the density difference δ_ρ for the cylinder (solid line, $\nu = 0$) and the sphere (dashed line, $\nu = 1$).

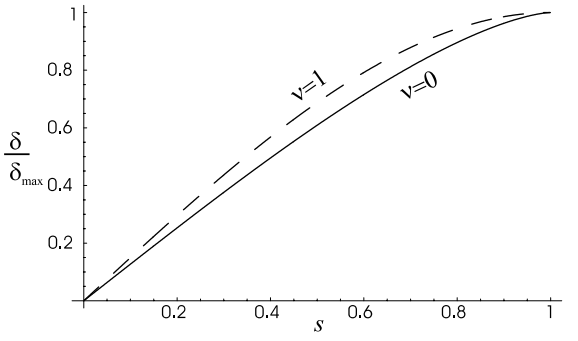

Fig. 7. The normalised elongation of the capsule radius δ/δ_{max} during the melting in the cylinder (solid line, $\nu = 0$) and the sphere (dashed line, $\nu = 1$) vs the relative solid displacement, s.

which describes the effect of melting there, leads to higher relative decrease of the solid volume of the sphere, than that of the cylinder. Therefore the rate of swelling is initially higher for the sphere. To the end of the melting, however, when s tends to 1, the relative area of the contact surface is smaller of the sphere than for the cylinder, which leads to the lower rate of swelling of the sphere than that of the cylinder.

The main feature of the solution of the problem, is that, even if the chosen normalised difference between the solid and liquid densities, $\delta_\rho = 0.3$, is sufficiently large, the effect on the melting rate is smaller because the maximum elongation of the capsule radius, $\delta_{max} = \delta_\rho/(\nu+2) + O(\delta_\rho^2)$, which actually describes the effect of the swelling on the melting rate, is smaller than δ_ρ, and the formula for the melting rate (41) also includes the factor 1/4 at the first-order correction caused by the exponent 1/4 in the formula (39) for the melting rate. Therefore, even for the cylinder we have the first-order correction to the melting rate to be of order $\delta_\rho/8$, while the second order correction describing the error of the model will be about $\delta_\rho^2/16$. For the maximum value $\delta_\rho = 0.3$ the latter is less than 1%.

From the expression for the melting rate (39) it can be seen that the first-order correction to the melting with regard to Stefan number can be derived from the model linear in transversal temperature distribution by substitution $T_w(1 - 7SteT_w/20)$ for T_w. For $T_w = 1$ and $Ste = 0.1$ the first-order correction term is less than 5%, while the model error, being of order $O(Ste^2)$, is around 1%.

4. Conclusions

The analysis performed in this work led to a simplified model of contact melting process inside an elastic capsule of circular form. Using linearisation with regard to the Stefan number, a closed-form evolution equation for the solid core motion within the capsule is found, describing the influences of the melt convection and capsule's wall deformation during melting owing to the difference between the solid and liquid densities.

Generally, the melting rate of spherical capsules is higher than that of cylindrical ones due to the different ratio of their surface area to the volumes: the ratio is 1.5 times higher for the sphere than for the cylinder. As can be seen from the expression for the melting rate (39), the accounting for the convective heat transfer to order of $O(Ste^2)$ leads to the $(1 - 7SteT_w/20)^{-3/4}$ -fold decrease of the melting rate, which, for $Ste \approx 0.1$, $T_w = 1$, makes approximately a 5% correction. This decrease of the melting rate due to the accounting for the convection heat flow is caused by the presence of the cold liquid generated by melting and driven by the convection along the layer—the effect not taken into account by

considering the linear approximation for the temperature distribution across the layer.

As was shown by computations, the swelling of the capsule leads to the lower rate of melting due to flattening of the contact surface. This is because the flattening redistributes the high pressure supporting the solid over a larger area, thereby making the pressure lower, which, in turn, increases the molten layer thickness, and, consequently, decreases the heat transfer and the whole melting rate.

Because the maximum elongation of the capsule radius due to swelling is larger for a cylinder than for a sphere for the same density difference, which is again caused by the difference between the ratio of the capsule surface to its volume (it is smaller for the cylinder, thus causing a larger elongation of the radius necessary to comprise the additional volume), the slowing down of the melting due to the swelling is larger for the cylinder than for the sphere.

The error of this linearised model is estimated as $(\delta_\rho^2/16)$ (due to swelling) and $O(Ste^2)$ (due to the nonlinearity of the temperature distribution), which for the normalised density difference, $\delta_\rho = 0.3$, and the Stefan number, $Ste = 0.1$, is estimated around 1%, which is sufficient for engineering applications.

Considering the capsule's shell dynamics yields restrictions on the shell dimensions or its material constants guaranteeing its intactness and the circular form of the capsule at any stage of melting. In particular, the lower bound for the admissible shell thickness is derived; its minimum admissible value is inversely proportional to the tensile strength and the Young's modulus. The latter provides the perfect guidelines for the manufacturer concerning the right selection of capsule's material and its shell thickness in order to sustain circularity of the capsule and to avoid ruptures in swelling.

References

[1] T. Saitoh, K. Hirose, High Raleigh numbers solutions to problems of latent heat thermal energy storage in a horizontal cylinder capsule, ASME J. Heat Transfer 104 (1982) 545–553.

[2] D. Nicholas, Y. Bayazitoglu, Thermal storage of a phase-change material in a horizontal cylinder, in: Alternative Energy Sources 1, Hemisphere Publishing Corp., Washington, 1983, pp. 351–378.

[3] M. Bareiss, H. Beer, An analytical solution of the heat transfer process during melting of an unfixed solid phase change material inside a horizontal tube, Int. J. Heat Mass Transfer. 27 (1984) 739–746.

[4] F. Moore, Y. Bayazitoglu, Melting within a spherical enclosure, ASME J. Heat Transfer 104 (1982) 19–23.

[5] P.A. Bahrami, T.G. Wang, Analysis of gravity and conduction driven melting in a sphere, ASME J. Heat Transfer 109 (1987) 806–809.

[6] S.K. Roy, S. Sengupta, The melting process within spherical enclosure, ASME J. Heat Transfer 109 (1987) 460–462.

[7] S.A. Fomin, T.S. Saitoh, Melting inside a spherical capsule with non-isothermal wall, Int. J. Heat Mass Transfer 42 (1999) 4197–4205.

[8] S.A. Fomin, A.V. Wilchinsky, T.S. Saitoh, Close-contact melting inside an elliptic cylinder, J. Sol. Energ. Eng. 122 (4) (2000) 192–195.

[9] A. Bejan, Single correlation for theoretical contact melting results in various geometries, Int. Commun. Heat Mass Transfer 19 (1992) 473–483.

[10] S.A. Fomin, Mathematical model of heat and mass transfer processes in contact melting, J. Soviet Math. 61 (6) (1992) 2426–2438.

[11] S.A. Fomin, P.S. Wei, V.A. Chugunov, Contact melting by non-isothermal heating surface of arbitrary shape, Int. J. Heat Mass Transfer 38 (17) (1995) 3275–3284.

[12] L.D. Landau, E.M. Lifshiz, Theory of elasticity, Pergamon Press, Oxford, 1986.